Cell and organ transplantology
SCIENTIFIC JOURNAL
КЛІТИННА ТА ОРГАННА ТРАНСПЛАНТОЛОГІЯ | КЛІТИННА ТА ОРГАННА ТРАНСПЛАНТОЛОГІЯ

ORIGINAL RESEARCH
Cell and Organ Transplantology. 2026; 14(1):e2026141189
https://doi.org/10.22494/cot.v14-1.189

Reparative osteogenesis around magnesium-containing biodegradable implants in rabbit femoral bones

Movchan O.[1], Kotelyukh B.[1], Savosko S.[2], Grabovoy A.[2]
[1]*Shupyk National Healthcare University of Ukraine, Kyiv, Ukraine*
[2]*Bogomolets National Medical University, Kyiv, Ukraine*
**Corresponding author's e-mail: s.i.savosko@gmail.com*

Abstract

The demand for innovative biodegradable implants has stimulated the development of new manufacturing technologies. Implants made of biodegradable magnesium alloys demonstrate satisfactory biocompatibility; however, the characteristics of their biodegradation in body tissues, particularly in bone tissue, still require further investigation.

***Objective** – to investigate tissue reactions around magnesium alloy implants during the course of their biodegradation in rabbit femoral bones.*

***Materials and methods.** In an experimental rabbit model, a tunnel defect was created in the distal epiphysis of the femur, into which pins made of MZZ-P or MZZ-MB magnesium alloys were implanted. After 8 and 16 weeks, histological sections were examined to assess tissue reactions around the pins, including connective tissue responses, osteogenesis, and implant biodegradation within the bone.*

***Results.** Degradation of MZZ-P and MZZ-MB magnesium alloys in the femoral bone was observed, accompanied by elimination of inorganic material against the background of an inflammatory reaction. At 2 and 4 weeks, the signs of reactive connective tissue complex formation around both types of implants were similar, while osteogenesis had only begun. The dynamics of local osteogenesis at 8 and 16 weeks around MZZ-P and MZZ-MB implants depended on the microenvironment determined by the level of implant biodegradation. MZZ-P degraded less intensively; however, this did not result in enhanced osteogenesis compared with MZZ-MB. At 16 weeks, the specific density of bone tissue did not differ significantly between the groups (35.7 ± 7.6 % and 41.6 ± 1.2 %, respectively; $p = 0.12$). Osteogenesis significantly progressed between weeks 2 and 16, increasing 2.6-fold and 2.2-fold, respectively ($p < 0.001$).*

***Conclusions.** Around both MZZ-P and MZZ-MB implants in the femoral bone, an increase in the number of bone trabeculae occurred during alloy biodegradation. Implant characteristics (chemical composition and biodegradation rate) had less influence on osteogenesis than the time factor.*

***Keywords**: bone tissue; osteogenesis; bone implant; magnesium alloy; tissue reactions*

Introduction

In the modern world, an increasing number of biotechnological and bioengineering approaches aimed at tissue and organ regeneration are being developed [1]. This trend is particularly evident in the field of traumatology and orthopedics due to the sharp increase in the number of victims resulting from military conflicts and civilian industrial injuries. Throughout the development of traumatology and orthopedics, considerable efforts have been directed toward the search for effective methods of osteosynthesis [2] and the introduction of novel materials for implant manufacturing [3].

Historically, plates and screws made of medical-grade stainless steel and titanium alloys have been considered the gold standard of treatment [4]. These devices allow rapid restoration of the function of the injured limb [5]. However, the long-term success of surgery using conventional fixation devices remains challenging because of several drawbacks, including infectious complications, bone lysis at implant insertion sites caused by the significant difference in elastic modulus between the fixation device and bone tissue, leading to the "stress-shielding" effect that negatively affects blood supply around the fracture site [6], the risk of implant migration, and the need for repeated surgical intervention for implant removal [7,8].

To address problems at the interface of materials science and bioengineering, the use of biodegradable materials for bone fixation has been proposed [9]. Among the novel materials, magnesium alloys [10] have emerged as an innovative alternative to traditional metallic and inert polymer implants [11], intended for the fixation of bone fragments during fracture consolidation followed by gradual degradation [12]. Magnesium-based fixation devices demonstrate excellent biocompatibility and mechanical strength [13], while the structure of these materials promotes osseointegration [14], thereby minimizing adverse postoperative reactions [15]. Magnesium alloys exhibit sufficient mechanical strength combined with an adequate degradation rate in experimental animal models [16] and contribute to effective bone tissue regeneration. Furthermore, during biodegradation, the material decomposes into safe components that may subsequently be eliminated from the body without adverse effects [17]. The principal advantage of magnesium alloy implants is the elimination of the need for secondary surgery to remove fixation devices [18, 19].

Magnesium alloys are considered among the most promising biodegradable materials for fracture osteosynthesis [20, 21]. However, despite the aforementioned advantages, issues related to unpredictable degradation kinetics [22], mechanical strength, and biocompatibility still impose certain limitations on their implantation [14]. The degradation rate and osteogenic properties are difficult to control, which may adversely affect bone integration following implantation [23]. For a more comprehensive understanding of these issues, it is necessary to evaluate how innovative magnesium alloy materials can address the most common challenges and to identify potential obstacles to their clinical application depending on their composition, particularly alloying with magnesium diboride [24].

Objective – to investigate tissue reactions around magnesium alloy implants during the course of their biodegradation in rabbits.

Materials and methods

Bioethics. All animal procedures were performed in accordance with the bioethical standards of the EU Directive 2010/63/EU "On the protection of animals used for scientific purposes" and were approved by the Commission on Bioethical Expertise and Ethics of Scientific Research (Protocol No. 195 of the Bioethics Committee of Bogomolets National Medical University).

Characteristics of the implant. In this study, the magnesium alloy was produced using the spark plasma sintering (SPS) method on a KCE-FCT HP D 25-SD system (*FCT Systeme GmbH,* Germany). A powder mixture of ZK61 with 10 wt. % MgB_2 was placed into a graphite mold with a diameter of 20 mm. To prevent powder adhesion to the mold, the walls were insulated with 0.5 mm graphite foil. The sintering regime included preliminary compaction of the powder mixture to improve electrical conductivity. The sintering cycle involved heating to 600 °C at a rate of 100 °C/min under a pressing force of 16 kN. The holding time at the isothermal temperature was 10 min. Cooling occurred under residual pressure.

The incorporation of MgB_2 additives into the powder alloy composition promoted the formation of a denser and more stable passive layer on the alloy surface upon contact with the biological environment. Such a layer hindered further magnesium dissolution.

Animal model. A tunnel defect 2 mm in diameter and 13 mm in length was created at the level of the distal femoral epiphysis in 16 male rabbits (mean body weight 2.25 kg, age 10–12 months) [25]. Immediately after defect creation, a sterile MZZ-P pin (magnesium ZK61) was implanted into the epiphysis of the left femur, whereas an MZZ-MB pin (magnesium with 8 wt. % MgB_2) was implanted into the right femur. All animal manipulations were performed under intraperitoneal anesthesia with thiopental sodium at a dose of 50 mg/kg (*Arterium*, Ukraine). At 2, 4, 8, and 16 weeks, four animals at each time point were euthanized by administration of a lethal dose of anesthesia, and bone samples were collected for histological examination.

Histological examination. Bone samples were fixed in a 10 % formalin solution (*Chimlaborreactiv*, Ukraine). Demineralization was performed in a 7 % EDTA solution (*Thermo Fisher Scientific*, USA). After dehydration in graded alcohols, the samples were embedded in paraffin Surgipath Paraplast Regular (*Leica*, Germany) [26]. Sections 10 μm thick were prepared using a Thermo Microm HM 360 microtome (*Thermo Fisher Scientific*, USA) and stained with hematoxylin and eosin.

Histological specimens were examined using a BX51 light microscope, and images were captured with a C3040ZOOM digital camera using DP-Soft 3.2 software (all – *Olympus*, Japan). Bone tissue density (%) around the tunnel defect was measured within a distance of up to 500 μm from the canal perimeter using the ImageJ 1.46 image analysis system (64-bit Java 1.8.0_172; *Wayne Rasband*, NIH, USA). For this purpose, a mask composed of multiple microphotographs from each sample was generated, enabling the evaluation of 1/2 to 3/4 of the defect perimeter.

Pin biodegradation was evaluated visually and microscopically using a semi-quantitative 4-point scoring system: 0 – intact; 1 – degradation up to 25 %; 2 – degradation up to 50 %; 3 – degradation of 75 % or more; 4 – complete degradation (absence of large fragments). At this stage of pin degradation, a fine-crystalline amorphous mass was detected within bone lacunae. The dynamics of inorganic mass accumulation were assessed using the following scoring system: 0 – absent; 1 – small focal accumulations; 2 – large or several accumulations; 3 – multiple accumulations of crystalline material (including beyond the defect perimeter).

Statistical analysis. Statistical analysis was performed using StatPlus (version 7.0) software (*AnalystSoft Inc*., USA) and the RStudio development environment (version 2026.01.0+392) (*Posit Software*, USA). Data distribution normality was assessed using the Shapiro-Wilk test. Differences between groups and the effect of time were evaluated using two-way analysis of variance (two-way ANOVA). Associations between variables were analyzed using Spearman's nonparametric correlation and linear regression analysis. Data are presented as mean ± standard error of the mean (Mean ± SEM). A value of $p \leq 0.05$ was considered statistically significant.

Results and discussion

Macroscopically, the implantation sites of the pins demonstrated signs of edema at the first observation time point; however, no edema was observed at later stages. Based on microscopic examination of femoral bone samples at the implantation site, the mean specific density of bone tissue was measured and compared with the dynamics of pin biodegradation. Pin degradation accompanied by the appearance of fine-crystalline material (hereafter referred to as implant derivatives) was detected. An analysis was performed to evaluate the relationship between the intensity of pin degradation and the type of magnesium alloy (Fig. 1).

The results of two-way analysis of variance (two-way ANOVA) indicated that the group factor showed a pronounced tendency toward differences in implant degradation intensity, particularly for implants manufactured from MZZ-MB ($p = 0.05$). The dynamics of implant degradation significantly progressed between weeks 2 and 16 ($p = 0.004$). Microscopically, degradation of MZZ-MB implants was somewhat greater than that of MZZ-P implants; however, the overall characteristics of this process were similar for both implant types ($p = 0.91$).

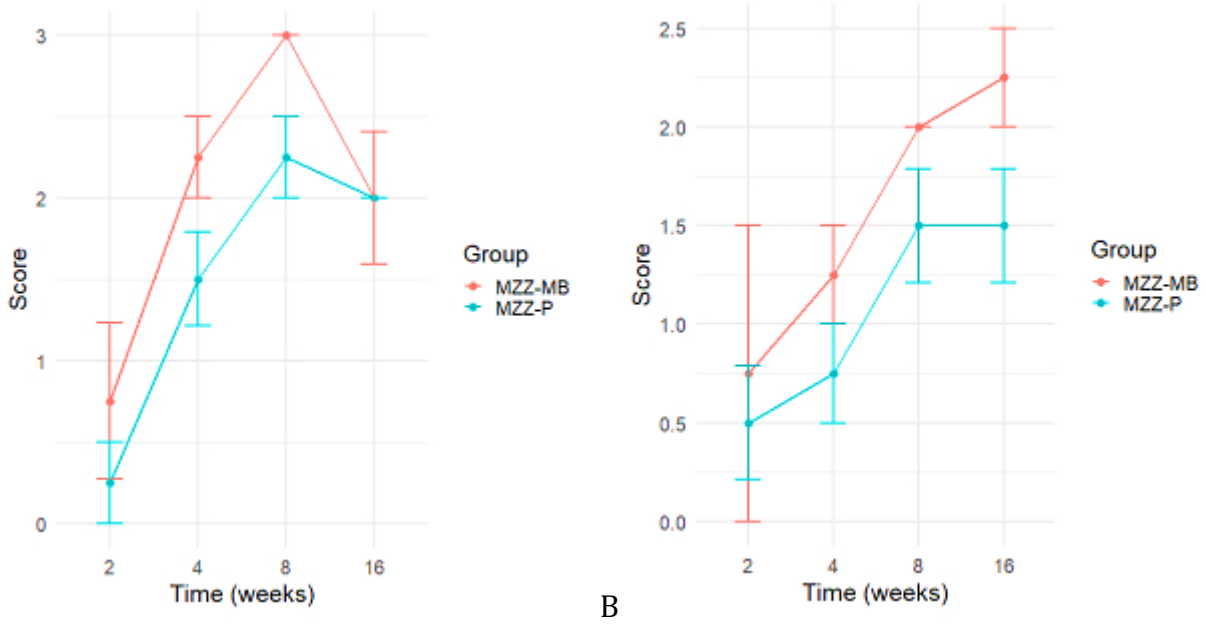

Fig. 1. *Dynamics of pin degradation (A) and detection of fine-crystalline derivatives (B) in the rabbit femoral bones.*

The hypothesis of a linear relationship between pin degradation and time was evaluated. The degree of metallic pin degradation and local alloy dissolution with the release of its derivatives positively correlated with time (rho = 0.48, $p = 0.01$ and rho = 0.55, $p < 0.001$, respectively). Linear regression models including the time factor (experimental period) and the semi-quantitative scoring scale demonstrated a linear pattern of pin degradation ($\beta = 0.06$, 95 % CI 0.0–0.12; $p = 0.05$) and detection of its derivatives in bone samples ($\beta = 0.07$, 95 % CI 0.02-0.12; $p = 0.01$).

Histological examination at 2, 4, 8, and 16 weeks after implantation of MZZ-P and MZZ-MB pins demonstrated that, as degradation progressed and fine-crystalline magnesium alloy derivatives appeared, signs of an inflammatory response and foci of connective tissue complex (capsule) formation with characteristic temporal dynamics were observed. Two weeks after implantation, a thin layer of newly formed connective tissue was detected along almost the entire perimeter of the tunnel defect. This tissue was characterized by inflammatory

infiltration, newly formed thin-walled blood vessels, fibroblasts, and a moderate amount of collagen fibers.

Variability in the condition of the connective tissue capsule around the implant, both in terms of volume and intensity of inflammatory infiltration, depended on the local microenvironment. In areas where the implant was in close contact with bone trabeculae over a considerable distance, regions of the capsule with small thickness, minimal signs of cellular inflammatory infiltration, and higher collagen density were observed. In contrast, areas contacting foci of red bone marrow were substantially thicker and demonstrated pronounced inflammatory infiltration, increased density of newly formed microvessels, and, simultaneously, a lower content of collagen fibers. In these regions, slightly greater degradation of MZZ-MB implants compared with MZZ-P implants was noted. A greater number and larger areas containing metallic implant derivatives, particularly in the MZZ-MB group, were also observed (Fig. 1).

At 4 weeks, an increase in the maturity of the connective tissue capsule formed around both MZZ-P and MZZ-MB implants was observed. In general, the newly formed connective tissue demonstrated a microscopic increase in the number of fibroblast-lineage cells and collagen fiber density. At the same time, the newly formed capsules were characterized by structural homogeneity in terms of both the thickness of the identified regions and the cellular density of the scar tissue. A substantial portion of the perimeter of the implantation track consisted of a thin layer of dense fibrous tissue with weakly expressed signs of inflammatory infiltration. However, local zones with more pronounced cellular inflammatory infiltration, a relatively thick layer of regenerating connective tissue, and blood microvessels were identified.

The volume of newly formed connective tissue and the intensity of inflammatory infiltration depended on the degree of implant biodegradation. In particular, pins manufactured from MZZ-MB underwent greater degradation, which was accompanied by more pronounced tissue reactions and a larger amount of cellular detritus. In cases of substantial implant degradation, the perimeter of the implantation track containing the implant underwent marked structural changes. In other cases, where inflammation and necrosis were less pronounced, signs of osteogenesis were observed. Microscopic manifestations of reparative osteogenesis included the appearance of thin bone trabeculae, a high density of osteoblasts along the trabecular perimeter, and close localization to the implantation track. The pattern of trabecular formation was highly variable and differed not only between samples within the groups but also depending on the tissue elements surrounding the implant. Thus, osteogenesis along the implant perimeter was heterogeneous.

At 8 weeks, histological variability became even more pronounced. Despite the increased osteogenic activity, confirmed by a greater specific density of newly formed bone tissue around the implant (Table 1), several adverse effects were also observed. Microscopically, an increased cellular inflammatory response to implant derivatives was detected, resulting in a greater amount of cellular detritus compared with week 4. Osteogenesis around MZZ-P implants was more homogeneous, whereas around MZZ-MB implants it differed substantially, demonstrating greater heterogeneity and variability. MZZ-MB implants generally underwent complete degradation or degradation exceeding 50 %. Reparative osteogenesis was heterogeneous, with newly formed bone trabeculae detected at the border of the implantation track; however, within the same sample, additional osteogenesis was also observed at some distance from the implant. Thus, as implant degradation progressed, not only local but also distant osteogenesis occurred.

At 16 weeks, fragments of pins manufactured from both MZZ-MB and MZZ-P were still detectable, although they had undergone marked degradation, and some had completely dissolved into a paste-like mass (Fig. 2). Foci of dead cells (cellular detritus and areas of

necrosis) and inflammatory infiltration were still present; however, the number and specific area of bone trabeculae were microscopically greater than at previous time points ($p < 0.001$) (Table 1), with no significant differences detected between implant types ($p = 0.12$). It should be noted that a similar trend was observed at the level of distantly located bone trabeculae. This may indicate that elimination of implant derivatives is associated not only with osteogenesis at the implant–tissue interface but also with distant osteogenesis.

To investigate the relationship between changes in bone tissue density and cellular reactions, an association analysis was performed between the amount of bone tissue along the perimeter of the pin implantation track and the experimental time point. A positive correlation was established between the duration of the experiment and the mean percentage of pin coverage by bone tissue (rho = 0.58; $p < 0.001$), indicating positive dynamics of osteogenesis around the implant. Two-way analysis of variance demonstrated a significant increase in bone tissue quantity throughout the experiment ($p < 0.001$); however, the dynamics between the two groups did not differ significantly ($p = 0.12$), nor did the perimeter of contact with bone trabeculae ($p = 0.66$) (Table 1).

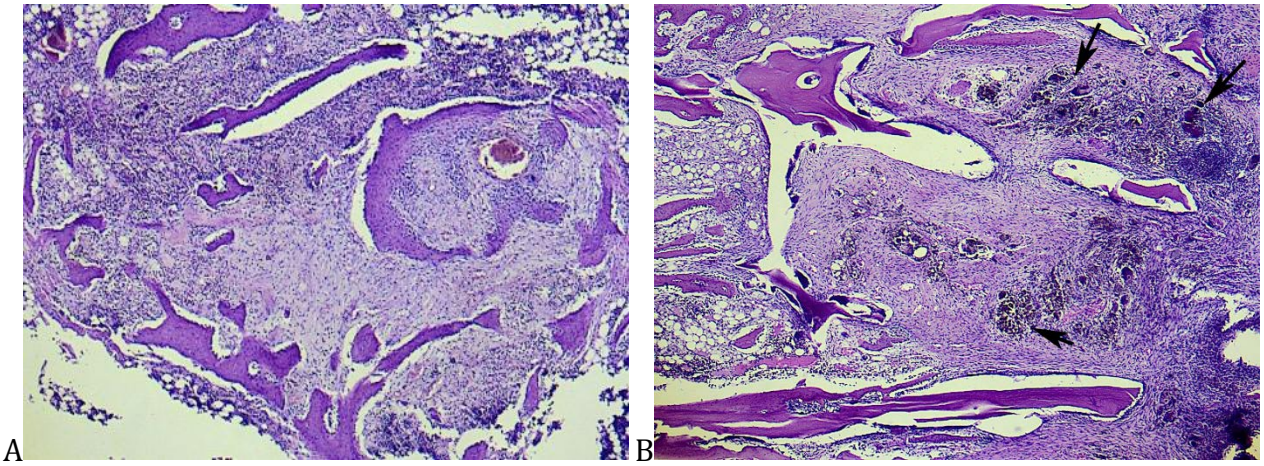

Fig. 2. *Microphotographs of histological sections of rabbit femoral bones 16 weeks after implantation of MZZ-P (a) or MZZ-MB (b) pins into the femur: bone trabeculae along the defect perimeter; the defect is replaced by scar tissue containing implant derivatives (arrow). Light microscopy, hematoxylin and eosin staining, ×40 magnification.*

Table 1. *Specific density of bone tissue around implants, %.*

Group / implant type	Term				Two-way ANOVA
	2 weeks	4 weeks	8 weeks	16 weeks	
MZZ-P	13.6 ± 1.9	32.6 ± 3.4	36.2 ± 8.5	35.7 ± 7.6	$p_1 < 0.001$
MZZ-MB	19.1 ± 0.9	29.9 ± 2.8	21.7 ± 4.5	41.6 ± 1.2	$p_2 = 0.12$
Mean value for implants	16.3 ± 1.31	31.3 ± 2.10	28.9 ± 5.2	38.7 ± 3.7	$p_3 = 0.66$

Note: p1 – time factor; p2 – group factor; p3 – interaction between time and group factors.

At the same time, a statistically significant inverse relationship was observed between the amount of bone tissue and the presence of implant derivatives at 4 weeks ($p = 0.02$), with a tendency toward such an association at 16 weeks ($p = 0.07$) (Table 2). These findings indicate that tissue reactions around the implant, including reparative osteogenesis, represent a complex and multifactorial phenomenon in injured bone, where the formation of lacunae may occur but does not necessarily determine the outcome of regeneration, whereas rapid implant degradation negatively affects bone tissue density

Table 2. *Results of the linear regression model evaluating bone tissue percentage and the implant derivative factor.*

Independent variable – % of bone tissue	Regression coefficient, β	SE	95 % CI		t	p-value
			LCL	UCL		
2 weeks	0.16	1.59	-4.26	4.58	0.10	0.93
4 weeks	-8.90	2.72	-15.56	-2.23	-3.26	0.02
8 weeks	3.54	6.58	-12.55	19.64	0.54	0.61
16 weeks	-21.41	9.71	-45.18	2.36	-2.20	0.07

Thus, the development of biodegradable resorbable implants is of considerable practical interest. Magnesium-containing alloys are promising materials for implant manufacturing due to their temporary mechanical strength, resistance to organic compounds, relatively slow degradation, and relatively non-toxic biocompatibility. In the present animal study, the biodegradation dynamics of MZZ-MB and MZZ-P implants, differences in degradation intensity, and tissue reactions to the appearance of implant derivatives were demonstrated. We confirmed previously reported findings regarding the susceptibility of magnesium-based alloys to accelerated and localized corrosion followed by implant destruction [27-29].

The results indicate that the structural integrity of MZZ-MB and MZZ-P implants exhibits relatively limited corrosion resistance over time, whereas reparative bone tissue regeneration proved to be more prolonged than expected. Such discrepancies between these two factors in damaged bone may become a substantial obstacle to successful bone healing. Surface modification of magnesium alloys appears promising for improving biodegradation characteristics, biocompatibility, and biomechanical properties of implants [30]. Overall, the development of osteosynthesis implants based on advanced magnesium alloy manufacturing technologies has considerable potential in traumatology and orthopedics because of their favorable biomechanical characteristics and ability to degrade within tissues.

Conclusions

1. Implants made of magnesium MZZ-P and magnesium–borate alloy MZZ-MB undergo progressive degradation in the bodies of experimental animals, with MZZ-MB degrading relatively faster.
2. Around the implant, the initial development of a connective tissue capsule occurs, while the amount of cancellous bone tissue increases dynamically between 2 and 16 weeks of observation. An increase in the number of bone trabeculae around the implant was observed.
3. Faster biodegradation of the MZZ-MB implant compared with the MZZ-P implant did not result in a significant increase in osteogenesis around the magnesium–borate-containing pin. The time factor appeared to be a more significant determinant of osteogenesis than modification of the magnesium implant with magnesium borate.

AUTHOR CONTRIBUTIONS. *Conceptualization: M. O., K. B.; Methodology: K. B.; Investigation: K. B., S. S.; Formal analysis: M. O., G. A.; Writing – original draft: K. B.; Writing – review & editing: M. O., K. B., S. S., G. A. All authors approved the final manuscript.*

ARTIFICIAL INTELLIGENCE (AI) USAGE DECLARATION.
The authors declare that no artificial intelligence (AI) tools or generative AI technologies were

used in the writing, preparation, analysis, figure creation, or editing of this manuscript. All scientific content was developed exclusively by the authors.

CONFLICT OF INTEREST STATEMENT. *The authors declare that they have no conflicts of interest related to the research, authorship, and/or publication of this article.*

Received: March 4, 2026
Accepted: May 20, 2026
Published online: May 30, 2026

References

1. Hoang VT, Nguyen QT, Phan TTK, Pham TH, Dinh NTH, Anh LPH, et al. Tissue Engineering and Regenerative Medicine: Perspectives and Challenges. MedComm. 2025; 6(5):e70192. https://doi.org/10.1002/mco2.70192
2. Cheng HY, Liang CW, Wang JH, Kuo YR, Ko PY, Chuang CH, et al. The effects of augmentation choices for locking plate fixation in proximal humerus fracture osteosynthesis: a systematic review and meta-analysis. J Orthop Traumatol. 2025;26(1):47. https://doi.org/10.1186/s10195-025-00852-z
3. Wang JL, Xu JK, Hopkins C, Chow DH, Qin L. Biodegradable Magnesium-Based Implants in Orthopedics-A General Review and Perspectives. Adv Sci (Weinheim, Baden-Wurttemberg, Germany). 2020; 7(8):1902443. https://doi.org/10.1002/advs.201902443
4. Marin E, Lanzutti A. History of metallic orthopedic materials. Metals. 2025; 15(4):378. https://doi.org/10.3390/met15040378
5. Witte F. The history of biodegradable magnesium implants: a review. Acta Biomater. 2010; 6(5):1680–1692. https://doi.org/10.1016/j.actbio.2010.02.028
6. Misir A. Current developments in orthopaedic implant technology. J Orthop Surg Res. 2025; 20(1):927. https://doi.org/10.1186/s13018-025-06279-w
7. Hu J, Shao J, Huang G, Zhang J, Pan S. In Vitro and In Vivo Applications of Magnesium-Enriched Biomaterials for Vascularized Osteogenesis in Bone Tissue Engineering: A Review of Literature. J Funct Biomater. 2023; 14(6):326. https://doi.org/10.3390/jfb14060326
8. Luo Y, Wang J, Ong MTY, Yung PS, Wang J, Qin L. Update on the research and development of magnesium-based biodegradable implants and their clinical translation in orthopaedics. Biomater Transl. 2021; 2(3):188–196. https://doi.org/10.12336/biomatertransl.2021.03.003
9. Nasr Azadani M, Zahedi A, Bowoto OK, Oladapo BI. A review of current challenges and prospects of magnesium and its alloy for bone implant applications. Prog Biomater. 2022; 11(1):1-26. https://doi.org/10.1007/s40204-022-00182-x
10. Xu L, Ye L, Wang J, Qiu X. Magnesium-based alloys for bone regeneration and beyond: A review of advances and therapeutic prospects. Regen Ther. 2025; 30:977-983. https://doi.org/10.1016/j.reth.2025.10.010
11. Hassan N, Krieg T, Zinser M, Schröder K, Kröger N. An overview of scaffolds and biomaterials for skin expansion and soft tissue regeneration: insights on zinc and magnesium as new potential key elements. Polymers (Basel). 2023;15(19):3854. http://doi.org/10.3390/polym15193854
12. Chen L, Han J, Guo C. Research status and prospects of biodegradable magnesium-based metal guided bone regeneration membranes. Hua Xi Kou Qiang Yi Xue Za Zhi. 2024; 42(4):415-425. English, Chinese. https://doi.org/10.7518/hxkq.2024.2024140

13. Liu Y, Yin J, Zhu G-Z. Advances in magnesium-based biomaterials: strategies for enhanced corrosion resistance, mechanical performance, and biocompatibility. Crystals. 2025; 15(3):256. https://doi.org/10.3390/cryst15030256
14. Wen Z, Lei L, Zhang H, Jin Z, Shan Z, Liu W, et al. Magnesium-containing implants enhance bone healing: A mechanobiological perspective. Mechanobiol Med. 2025; 3(4):100161. https://doi.org/10.1016/j.mbm.2025.100161
15. Liu B, Yang J, Zhang X, Yang Q, Zhang J, Li X. Development and application of magnesium alloy parts for automotive OEMs: A review. J Magnes Alloys. 2023; 11:15–47. https://doi.org/10.1016/j.jma.2022.12.015
16. Kim J, Jung Y, Lee YS, Choi SW, Hwang G, Yun K. Micro-CT and Histomorphometric Analysis of Degradability and New Bone Formation of Anodized Mg-Ca System. Biomimetics (Basel). 2025; 10(9):583. https://doi.org/10.3390/biomimetics10090583
17. Shen Z, Zhou X, Zhao M, Li Y. A Structural Optimization Framework for Biodegradable Magnesium Interference Screws. Biomimetics (Basel). 2025; 10(4):210. https://doi.org/10.3390/biomimetics10040210
18. Hung CH, Kwok YC, Yip J, Wong HH, Leung YY. Bioabsorbable magnesium-based materials: potential and safety in bone surgery: a systematic review. CMTR. 2025; 18(2):24. https://doi.org/10.3390/cmtr18020024
19. Meng X, Liu A, Wu C, Han X, Yang Q, Qiu H, et al. Research Progress of Magnesium Alloys and Its Alloys in Medical Applications. Int J Gen Med. 2025;18:7101-7126. https://doi.org/10.2147/IJGM.S565096
20. Li G, Zhang L, Wang L, Yuan G, Dai K, Pei J, et al. Dual modulation of bone formation and resorption with zoledronic acid-loaded biodegradable magnesium alloy implants improves osteoporotic fracture healing: An in vitro and in vivo study. Acta Biomater. 2018; 65:486–500. https://doi.org/10.1016/j.actbio.2017.10.033
21. Aikin M, Shalomeev V, Kukhar V, Kostryzhev A, Kuziev I, Kulynych V, et al. Recent Advances in Biodegradable Magnesium Alloys for Medical Implants: Evolution, Innovations, and Clinical Translation. Crystals. 2025; 15(8):671. https://doi.org/10.3390/cryst15080671
22. Jia H, Li Y, Xu S, Xi Y, Gui W. Investigation of Degradation Behavior and Mechanical Performance Deterioration of Magnesium Alloys in Hank's Solution. Materials (Basel). 2025; 18(22):5102. https://doi.org/10.3390/ma18225102
23. Wang Z, Liu B, Yin B, Zheng Y, Tian Y, Wen P. Comprehensive review of additively manufactured biodegradable magnesium implants for repairing bone defects from biomechanical and biodegradable perspectives. Front Chem. 2022; 10:1066103. https://doi.org/10.3389/fchem.2022.1066103
24. Kotelyukh B A, Movchan O, Teslia S, Shtonda D. Prospects of osteosynthesis with fixators based on magnesium alloys, mechanical and physiological properties. The state of the problem at the current stage. Wiadomosci lekarskie. 2025; 78(1):162–167. https://doi.org/10.36740/WLek/197141
25. Lin Y-K, Wang H-W, Wu P-K, Lin C-L. Platelet-rich fibrin synthetic bone graft enhances bone regeneration and mechanical strength in rabbit femoral defects: micro-CT and biomechanical study. Journal of Functional Biomaterials. 2025; 16(8):273. https://doi.org/10.3390/jfb16080273
26. Wehrle E, Günther D, Mathavan N, Singh A, Müller R. Protocol for preparing formalin-fixed paraffin-embedded musculoskeletal tissue samples from mice for spatial transcriptomics. STAR Protoc. 2024; 5(2):102986. https://doi.org/10.1016/j.xpro.2024.102986

27. Antoniac I, Manescu Paltanea V, Antoniac A, et al. Magnesium-based alloys with adapted interfaces for bone implants and tissue engineering. J Regen Biomater. 2023; 10:rbad095. https://doi.org/10.1093/rb/rbad095
28. Chow DHK, Wang J, Wan P, et al. Biodegradable magnesium pins enhanced the healing of transverse patellar fracture in rabbits. Bioact Mater. 2021; 6(11):4176–4185. https://doi.org/10.1016/j.bioactmat.2021.03.044
29. Gao M, Na D, Ni X, et al. The mechanical property and corrosion resistance of Mg-Zn-Nd alloy fine wires in vitro and in vivo. Bioact Mater. 2021; 6(1):55–63. https://doi.org/10.1016/j.bioactmat.2020.07.011
30. Chaudhari Y S, Chaudhari M Y, Gholap A D, Alam M I, Khalid M, Webster T J, et al. Surface engineering of nano magnesium alloys for orthopedic implants: a systematic review of strategies to mitigate corrosion and promote bone regeneration. Front Bioeng Biotechnol. 2025; 13:1617585. https://doi.org/10.3389/fbioe.2025.1617585